QUANTUM STATE SWAPPING IN OPTICAL QUANTUM COMMUNICATION USING MACH–ZEHNDER INTERFEROMETER

Shamsolah Salemian* and Shahram Mohammad Nejad

Nanoptronics Research Center
Electrical and Electronics Engineering Department
Iran University of Science and Technology
Narmak, Tehran, Iran

الخلاصـة:

تتطلب الاتصالات الكمية بعيدة المدى عملية تبادل الحالة الكمية. وتعتمد طريقة مسح الحالة الكمية على التحكم الكمي المنطقي من نوع NOT (CNOT) أو المؤثرات الكمية المماثلة التي يصعب تطبيقها عملياً. وسوف نعرض - في هذه الورقة - نمطاً يمكن تطبيقه عملياً يعتمد على دائرة ضوئية ثنائية البعد (PLC) ، وذلك باستخدام مطياف ماك – زينهدر التداخلي. وقد مكننا هذا الأسلوب الجديد من تحديد عرض دليل الموجة وطول بوابة CONT على النحو التالي: 12 ميكرون و 3.8سم على التوالي.

*Corresponding Author:
E-mail: salemian@iust.ac.ir

Paper Received July 6, 2008; Paper Revised July 27, 2009; Paper Accepted October 1, 2009

ABSTRACT

Quantum state swapping is required for long-distance quantum communication. Quantum state swapping protocols are based on the quantum controlled-NOT (CNOT) or similar quantum logic operations, which are very difficult to implement experimentally. Here we present a feasible scheme for the implementation of quantum state swapping based on planar lightwave circuit (PLC) implementation of quantum CNOT gate. This quantum gate is realized by using the Mach–Zehnder interferometer. By using planar lightwave circuit in implementation, the width of waveguides and the length of CNOT gate were 12 microns and 2.8 cm, respectively.

Key words: quantum CNOT gate, quantum communication, entanglement swapping, quantum repeater, PLC

QUANTUM STATE SWAPPING IN OPTICAL QUANTUM COMMUNICATION USING MACH–ZEHNDER INTERFEROMETER

1. INTRODUCTION

Quantum state swapping is used in quantum computation and long-distance quantum communication [1]. Storage, transmission, and transformation of quantum states are basic procedures in quantum information processing and quantum computing. Photons are considered the best carriers for transmitting quantum information, whilst atoms can be used as "quantum memory" to store qubits. Any interaction of two subsystems can generate a compound state of a combined system [2].

Recently and increasingly, investigations have explored the possibilities of performing quantum state swapping in linear optics and solid state materials. Based on linear optic elements, a scheme was presented to perform entanglement swapping with intense, pulsed, quadrature entangled beams using direct detection [3]. An optical fiber entanglement source with bright, pulsed light [4] and some optical component, such as polarization beam splitter, half-wave plate, or 50:50 beam splitter, were used in this experiment [3, 4]. By using a class of qubit networks with on-site Coulomb interaction, it is possible to perform quantum state swapping between two distant electrons with opposite spins [5].

So far, no quantum state swapping based on planar lightwave circuit technology for integrated optics has been reported. The proposed method has the potential of being more compact and easily realized compared to linear optics implementation and is suitable for integrated optics.

The impossibility of isolating a physical system completely from its environment represents a major difficulty in the experimental realization of quantum information processing devices [6]. Quantum decoherence is created due to interaction between quantum system and its environment. A quantum repeater is used to overcome the decoherence problem in long distance quantum communication. Quantum repeaters are very important in quantum communication and quantum information processing due to their relevance in extending the distance of quantum key distribution, and as resources of entanglement over long distances, which, for example, may be used in quantum teleportation or quantum computer networks. The quantum repeaters perform a unitary transformation: given an input state, the entanglement properties of the state can be preserved for output at another physical location. The point is that the signal can become lost due to attenuation, scattering, or absorption, or it can obtain errors, for example, due to depolarization or dispersion in an optical fiber. Quantum memories allow the creation of entanglement independently for each link. This entanglement can then be extended to the full distance using entanglement swapping [7]. The idea of the quantum repeater is analogous to the classical scheme for signal transmission: divide the channel into N segments through which a suitable threshold of signal- to-noise ratio (SNR) can be met so as to regenerate the information and send it along another segment of the channel. The basic process of quantum repeater involves entanglement generation, purification, and swapping [8].

2. QUANTUM STATE SWAPPING

It is possible to entangle two photons that have never interacted before by using two down-conversion sources and then subjecting one photon from each entangled pair to a Bell-state measurement. This causes the other two photons, which have never interacted, to become entangled. Quantum state swapping can be achieved by cascading three quantum controlled-NOT gates (Figure 1).

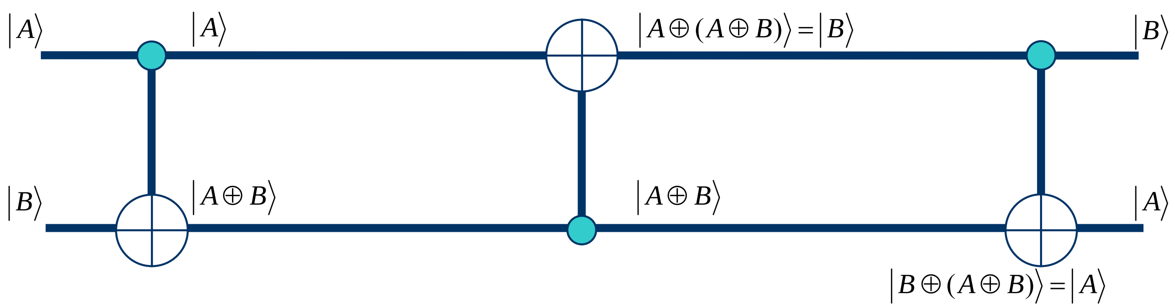

Figure 1. Schematic of quantum state swapping

From a practical point of view, the most important drawback of this scheme is that it requires the CNOT operation. Although certain quantum logic gates have been experimentally demonstrated in physical systems such as ion-traps [9] and high-finesse microwave cavities [10], up to now there has been no implementation of CNOT gates that could realistically be used for quantum swapping in the context of long-distance quantum communication. In the next section, a novel approach to implementation of quantum NOT and CNOT gates is presented. This implementation is based on planar lightwave circuit technology and is suitable for integrated optics. By using this CNOT gate, the general quantum state swapping method that does rely on the CNOT operation will be feasible.

3. QUANTUM STATE SWAPPING IMPLEMENTATION

The basic Mach–Zehnder interferometer is shown in Figure 2. In this device, a single input is split between two waveguides. The spacing of the waveguides is so that evanescent coupling does not take place.

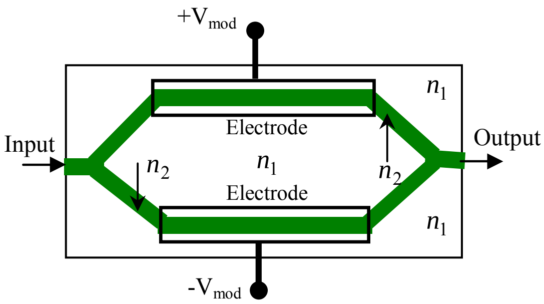

Figure 2. Mach-Zehnder interferometer

The two outputs are added together in a single output guide where the two waves interfere, with the amount of interference depending upon the difference in propagation time along the two limbs. The propagation constant of the two guides can be changed differentially by using the electro-optic effect to change the guide refractive indices. A DC bias can be applied to equalize the phase difference of the two limbs in the absence of a modulation voltage. An interferometric modulator using $LiNbO_3$ with bandwidths up to 40 GHz has been reported and it has a considerable future in optical communication and computation [11]. The transfer function matrix of this element is

$$U = \begin{bmatrix} \cos(\frac{\phi}{2}) & j\sin(\frac{\phi}{2}) \\ j\sin(\frac{\phi}{2}) & \cos(\frac{\phi}{2}) \end{bmatrix} \tag{1}$$

where ϕ is the phase difference between the two limbs of the modulator that adjust by applied voltage. Another way of producing phase difference between the two limbs of the modulator is by using a Kerr-like nonlinear waveguide. In the Kerr-like medium, the intensity of electromagnetic fields changes the refractive index of the waveguide and provides phase shift.

3.1. Implementation of Quantum NOT Gate

Qubits can be realized by two normal modes of dual-mode waveguides, such as the zero logical state $|0\rangle$ encoded into one normal mode, TM_0, and the logical one $|1\rangle$ given by other orthogonal normal mode, TM_1 (Figure 3). A qubit's state space consists of all superpositions of the basic normal modes $|0\rangle$ and $|1\rangle$.

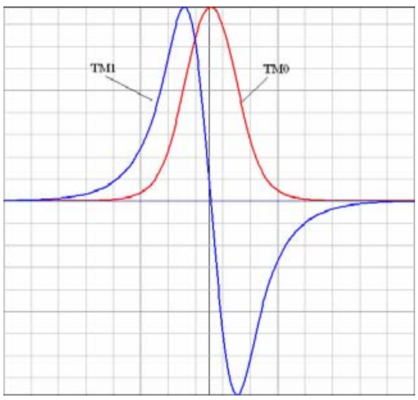

Figure 3. Electric-field profiles for TM0 and TM1 modes

As mentioned above, in this paper, an all-optical method is proposed for implementation of quantum gates. Realization of quantum NOT gate using Mach–Zehnder interferometer is shown in Figure 4. By applying the suitable V_{mod} to the electrodes, we can adjust the phase difference between the two limbs of the modulator.

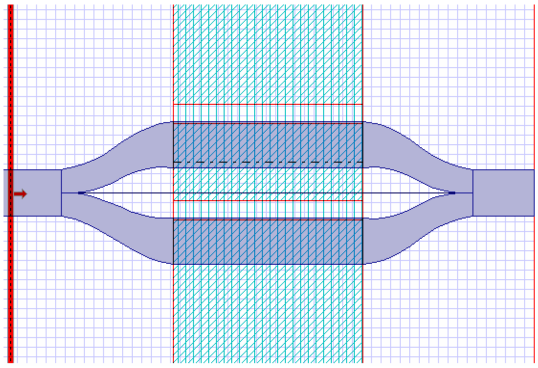

Figure 4. Realization of quantum NOT gate using Mach–Zehnder interferometer

With due attention to Equation (1), the relation between input and output of Mach–Zehnder interferometer is

$$\begin{bmatrix} |\psi_1\rangle \\ |\psi_2\rangle \end{bmatrix}_{out} = \begin{bmatrix} \cos(\frac{\phi}{2}) & j\,\sin(\frac{\phi}{2}) \\ j\,\sin(\frac{\phi}{2}) & \cos(\frac{\phi}{2}) \end{bmatrix} \begin{bmatrix} |0\rangle \\ |1\rangle \end{bmatrix}_{in} \quad (2)$$

If $\phi = 0$, then all inputs are unchanged at the gate output, but if ϕ is adjusted to the value of π, the modulator acts as a quantum NOT gate. All inputs to $|0\rangle$ appear as the $|1\rangle$ output with an additional phase and vice versa. Superposition states are generated by adjusting the phase difference. For example, by choosing $\phi = \pi/2$, we have the following states:

$$\begin{aligned} |\psi_1\rangle &= \frac{1}{\sqrt{2}}\left(|0\rangle + j\,|1\rangle\right) \\ |\psi_2\rangle &= \frac{1}{\sqrt{2}}\left(j\,|0\rangle + |1\rangle\right) \end{aligned} \quad (3)$$

The beam propagation method (BPM) simulation results for quantum NOT gate are shown in Figures 5 and 6.

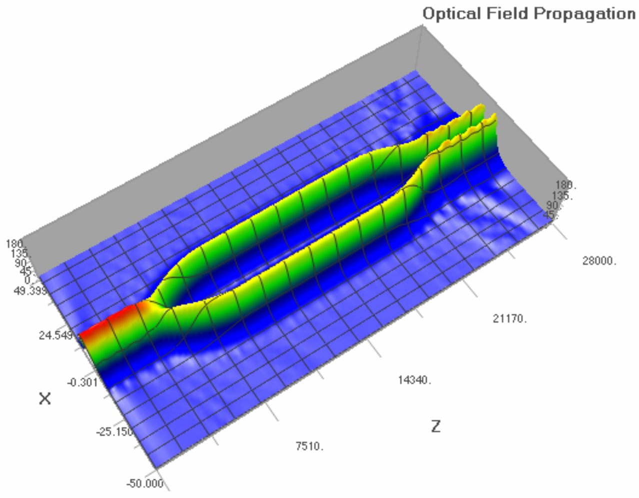

Figure 5. Quantum NOT: $|0\rangle \rightarrow |1\rangle$

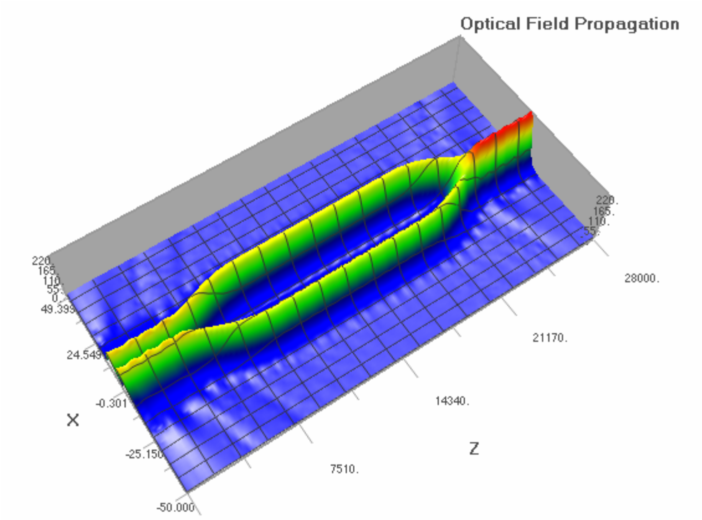

Figure 6. Q uantum NOT: $|1\rangle \to |0\rangle$

3.2. Implementation of Controlled NOT Gate

In the CNOT gate, if the input control bit is $|0\rangle$, then the control bit and the target bit do not change. In other cases, for input control bit $|0\rangle$, the target bit changes as below:

$$
\begin{array}{l} |0> \to |1> \\ |1> \to |0> \end{array} \tag{4}
$$

Both the coupled mode theory and the Mach–Zehnder interferometer are used for implementation of this gate. The planar lightwave integrated optics of this gate is shown in Figure 7. There is a coupling region in this scheme. The length of this coupler is designed for power transferring between two couplers for TM_1 mode. The electro-optic material, such as $LiNbO_3$, is used in the limbs of the modulator. Two electrodes are placed on two limbs. When the optical power is detected at the coupler output, the applied voltages on the electrodes are adjusted as the phase difference π is created between the two limbs of the modulator. If there is not any optical power on the output branch of the coupler, then the applied voltages on the electrodes are adjusted as the phase difference 0 is created between the two limbs of the modulator. When $|0\rangle$ is present at the control bit, the intensity of the qubit is never coupled into the output of the coupler. Therefore, the control and target qubits are left unchanged. When $|1\rangle$ is present at the control bit, the intensity of the qubit is coupled into the output of the coupler. Thus, a phase shift of π is created between the two limbs of the modulator and the states of the target bit will be flipped, namely $|0\rangle \to |1\rangle$ and $|1\rangle \to |0\rangle$.

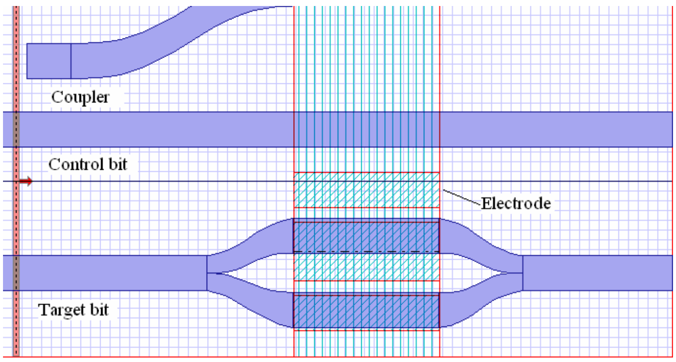

Figure 7. Controlled NOT gate realization. The width of waveguides is 12 µm. The length of coupler is 200µm, separation between coupler waveguides is 11 µm and gate length is 2.8 cm

The beam propagation method (BPM) simulation results for quantum CNOT gate are shown in Figures 8 to 11.

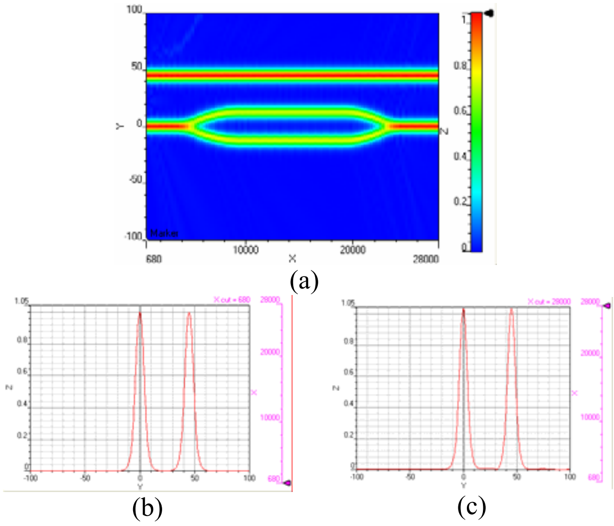

Figure 8. CNOT quantum gate: $|00\rangle \rightarrow |00\rangle$

(a) optical field amplitude, (b) input electric field profiles, (c) output electric field profiles

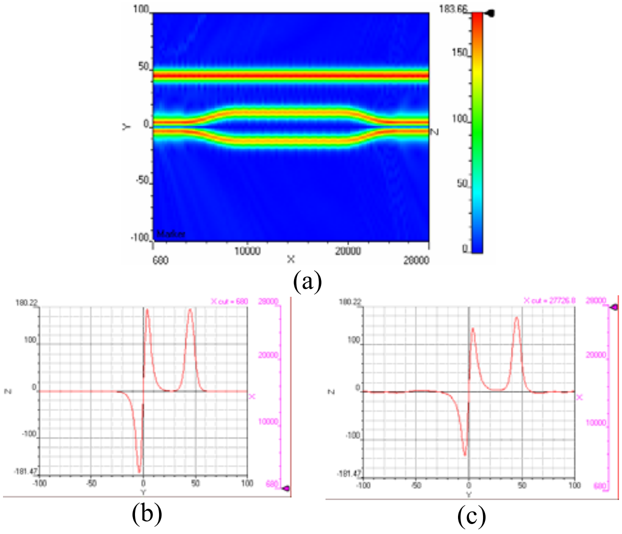

Figure 9. CNOT quantum gate: $|01\rangle \rightarrow |01\rangle$

(a) optical field amplitude, (b) input electric field profiles, (c) output electric field profiles

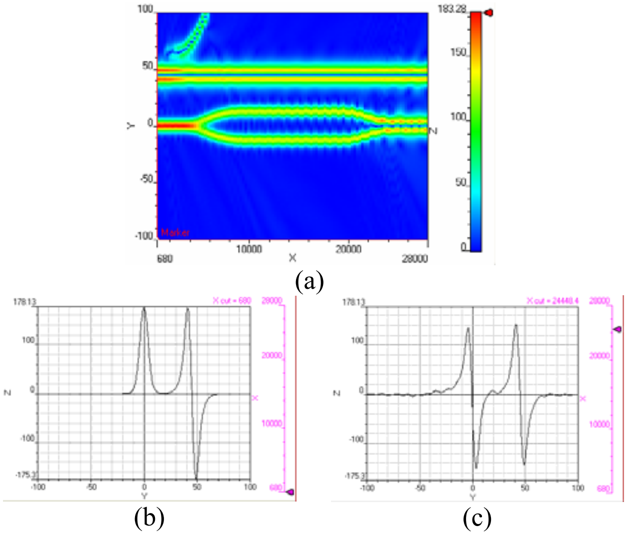

Figure 10. CNOT quantum gate: $|10\rangle \rightarrow |11\rangle$

(a) optical field amplitude, (b) input electric field profiles, (c) output electric field profiles

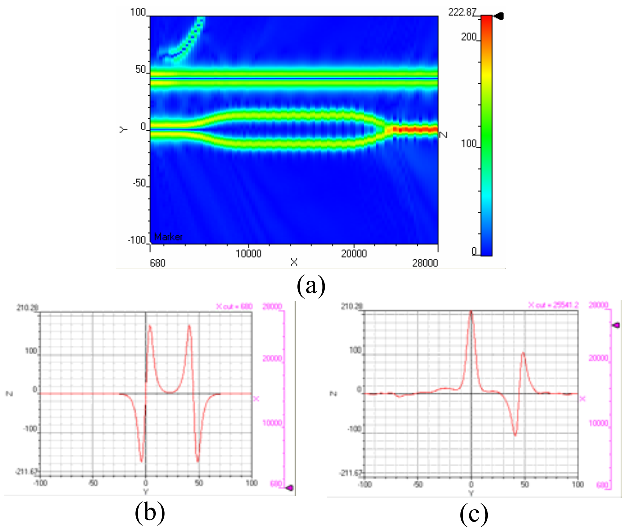

Figure11. CNOT quantum gate: $|11\rangle \rightarrow |10\rangle$

(a) optical field amplitude, (b) input electric field profiles, (c) output electric field profiles

3.3. Implementation of Quantum State Swapping

In this section, the scheme of quantum state swapping presented in Figure 1 is realized using three cascading controlled-NOT gates. Implemented quantum state swapping is shown in Figure 12. Simulation results are presented in Figure 13 and Figure 14. In Figure 13, states $|0\rangle$ and $|1\rangle$ have been applied to upper and lower branches, respectively. In the output of the scheme, states $|1\rangle$ and $|0\rangle$ appear in the upper and lower branches, respectively. These results show that quantum swapping has been performed successfully. Figure 14 shows the result for inverse states.

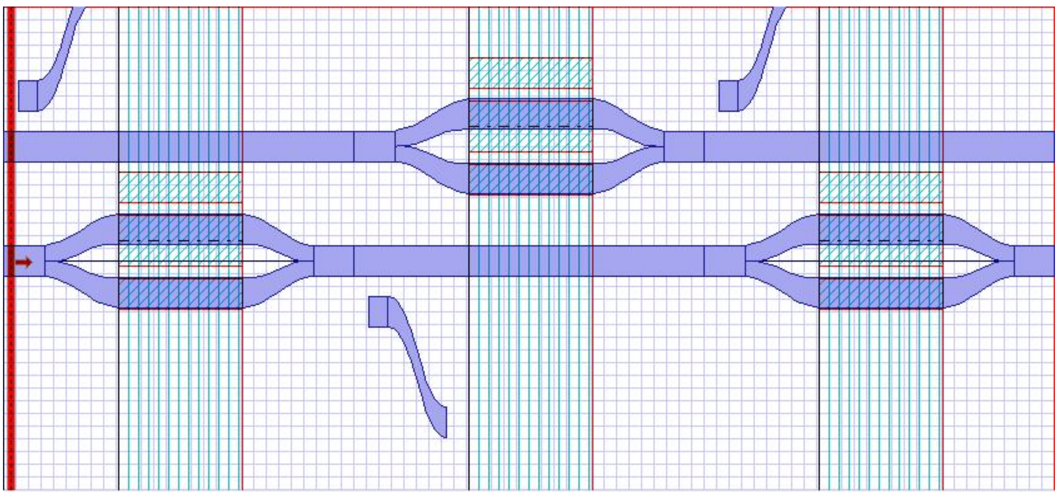

Figure 12. Implemented quantum state swapping

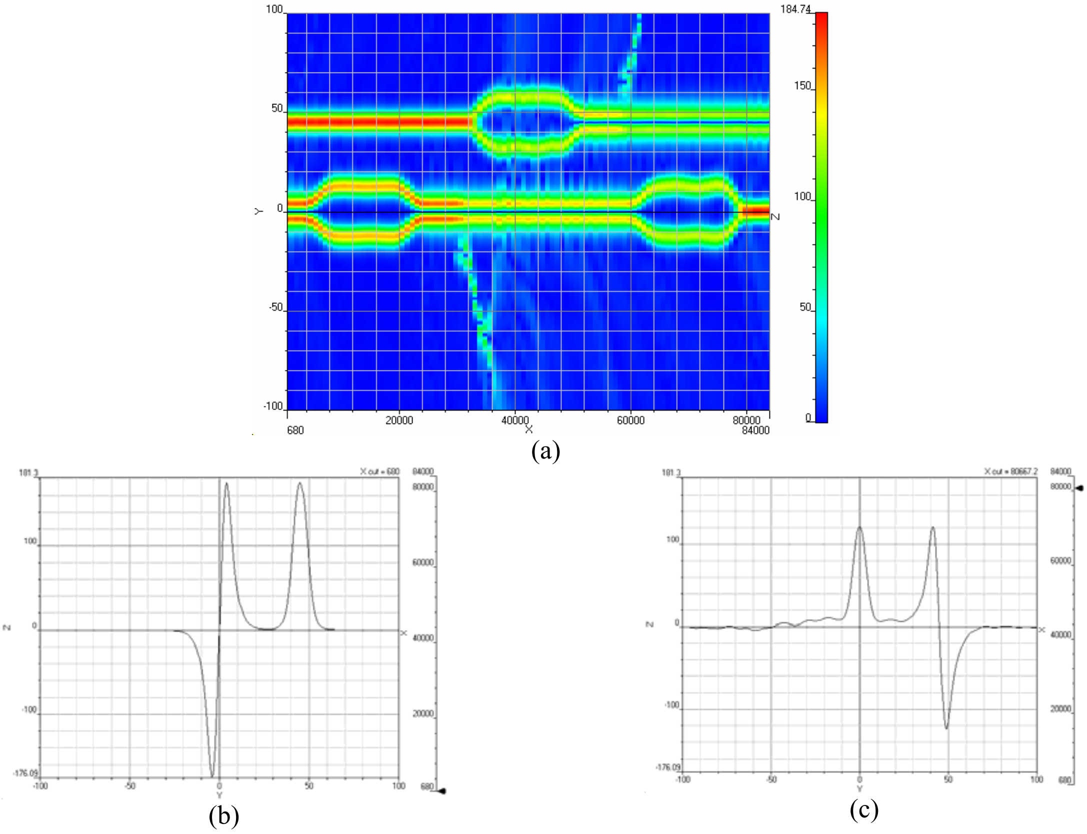

Figure 13. Quantum state swapping: $|01\rangle \rightarrow |10\rangle$

(a) optical field amplitude, (b) input electric field profiles, (c) output electric field profiles

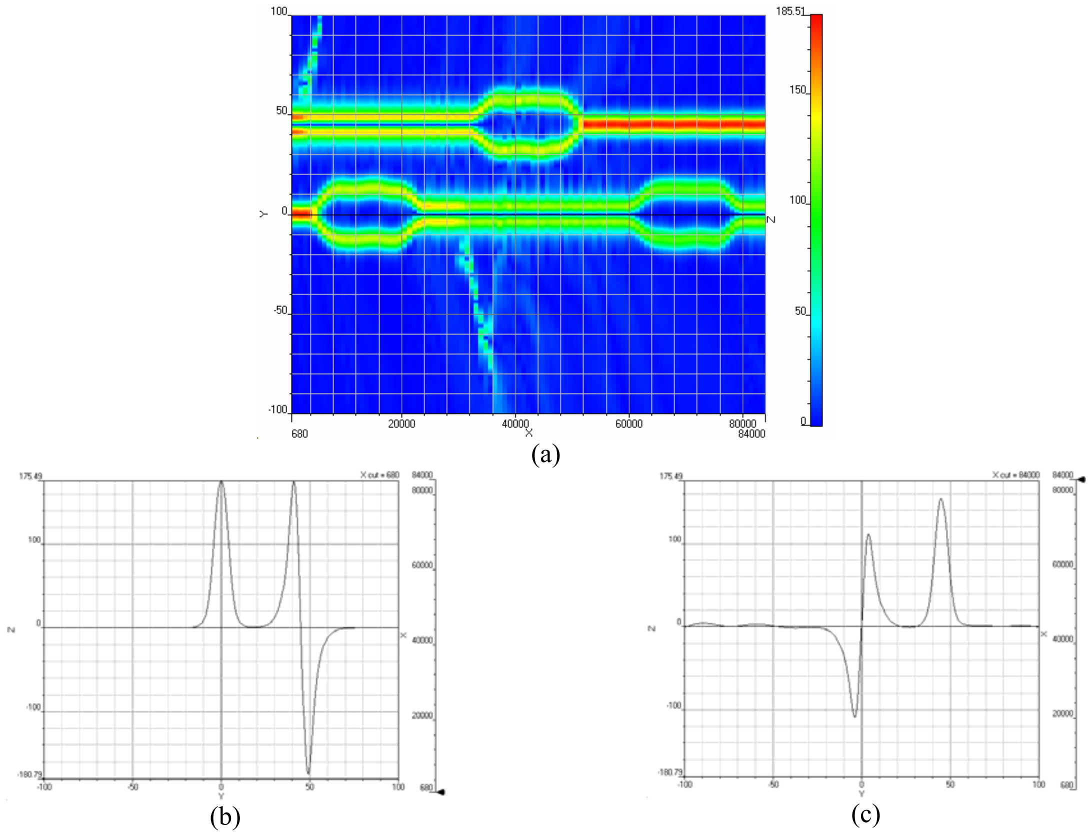

Figure 14. Quantum state swapping: $|10\rangle \rightarrow |01\rangle$

(a) optical field amplitude, (b) input electric field profiles, (c) output electric field profiles

4. CONCLUSION

In conclusion, we proposed an all-optical method for implementation of the quantum NOT and CNOT gates. By using planar lightwave technology, all single qubit and double qubit quantum logic gates are feasible. By using a dual mode waveguide Mach–Zehnder interferometer and directional couplers, we proposed a fully optical method to perform quantum NOT and CNOT gates as the basis of quantum state swapping.

REFERENCES

[1] M. Oskin, Frederic T. Chong, and Isaac L. Chuang, "A Practical Architecture for Reliable Quantum Computers", *IEEE Comp. Soc. Mag.,* **35(1)**(2002), pp. 79–87.

[2] C. H. Bennett, D. V. DiVincenzo, J. A. Smolin, and W. K. Wootters, "Mixed-State Entanglement and Quantum Error Correction", *Phys. Rev. A*, **54**(1996), pp. 3824–3851.

[3] O. Glock, S. Lorenz, C. Marquardt, J. Heersink, M. Brownnutt, C. Silberhorn, Q. Pan1, P. V. Loock, N. Korolkova, and G. Leuchs, "Experiment Towards Continuous-Variable Entanglement Swapping: Highly Correlated Four-Partite Quantum State", *Phys. Rev A*, **68**(2003), pp. 012319.1–012319.8.

[4] O. Glock, U. L. Andersen, and G. Leuchs, "Verifying Continuous-Variable Entanglement of Intense Light Pulses", *Phys. Rev A*, **73**(2006), pp. 012306.1–012306.15.

[5] S. Yang and Z. Song, "Quantum State Swapping Via a Qubit Network With Hubbard Interactions", *Phys. Rev B,* **73**(2006), pp. 195122.1–195122.6.

[6] E. Waks, A. Zeevi and Y. Yamamoto, "Security of Quantum Key Distribution With Entangled Photons Against Individual Attacks", *Phys. Rev. A*, **65**(2002), pp. 52310.1–52310.16.

[7] N. Gisin, G. Ribordy, W. Tittel, and H. Zbinden, "Quantum Cryptography", *Rev. Mod. Phys.,* **74**(2002), pp. 145–195.

[8] P. Kok, C. P. Williams, and Jonathan P. Dowling, "Construction of a Quantum Repeater With Linear Optics", *Phys. Rev. A*, **68**(2003), pp. 022301.1–022301.5.

[9] C. Monroe, D. M. Meekhof, B. E. King, W. M. Itano, and D. J. Wineland, "Demonstration of a Fundamental Quantum Logic Gate", *Phys. Rev. Lett.*, **75**(1995), pp. 4714–4717.

[10] A. Rauschenbeutel, G. Nogues, S. Osnaghi, P. Bertet, M. Brune, J. M. Raimond, and S. Haroche, "Coherent Operation of a Tunable Quantum Phase Gate in Cavity QED", *Phys. Rev. Lett.*, **83**(1999), pp. 5166–5169.

[11] T. Tamir, *Guided-Wave Optoelectronics*. New York: Springer-Veriag, 1988.